SHAPE EVOLUTION OF A LONG BUBBLE PENETRATING LIQUIDS WITH VARIOUS VISCOSITIES

Cheng-Hsing Hsu
Department of Mechanical Engineering, Chung-Yuan Christian University, Chung Li, Taiwan, R.O.C

Ching-Chuan Chang
Mechanical Engineering, Army Academy, Chung Li, Taiwan, R.O.C., nashsccc8142@yahoo.com.tw

Chia-Chuan Kuo
Department of Mechanical Engineering, Taoyuan Innovation Institute of Technology, Chung Li, Taiwan, R.O.C.

Kuang-Yuan Kung
Graduate School of Materials Applied Technology, Taoyuan Innovation Institute of Technology, Chung Li, Taiwan, R.O.C.

Follow this and additional works at: https://jmstt.ntou.edu.tw/journal

Part of the Engineering Commons

SHAPE EVOLUTION OF A LONG BUBBLE PENETRATING LIQUIDS WITH VARIOUS VISCOSITIES

Acknowledgements

SHAPE EVOLUTION OF A LONG BUBBLE PENETRATING LIQUIDS WITH VARIOUS VISCOSITIES

Cheng-Hsing Hsu[1], Ching-Chuan Chang[2], Chia-Chuan Kuo[3],

and Kuang-Yuan Kung[4]

ABSTRACT

This paper aims at the effect of gas flow and viscosity of the fluid on the profile of a long bubble. The gas flow controlled by a mass flow controller is injected into a tube filled with liquid silicon oil. The images of bubble profile are captured by a high-speed camera. The fractional converge of the liquid and the hollow ratio of the bubble is estimated by measuring the width of these images. The result shows that the values of Capillary number and Reynolds number increase as the gas flow rate increase under a constant viscosity. However, the hollow ratio decreases while the flow rate increases. The value of fractional converge is 0.6 while the value of Capillary number approaches to 10 for the 500cs silicon oil, the results are consistent with the projections of Cox.

I. INTRODUCTION

There are many applications on bubble research, such as marine and industrial applications. In marine applications, the laminar is separated by a bubble when torpedo launched by submarine. The friction of high-speed torpedo with the sea is reduced when the surface of the torpedo is wrapped up in the ellipsoidal bubble [6].

In the aspect of industrial applications, bubble is also applied to the processes of gas-assisted molding [7, 12]. The products manufactured by gas-assisted molding have many advantages, such as: the decreasing of the residual stress and warpage, the increasing of mechanical strength and cost reducing, etc.

The penetration by a long bubble of a Newtonian fluid in the horizontal tube has been studied for many years. Fairbrother and Stubbs [5] first studied the penetration of a long bubble in a tube filled with fluid and obtained anempirical formula relating the fractional coverage m and the capillary number Ca; the results showed that $m = Ca^{0.5}$ when Ca is within 10^{-5} and 10^{-2}. Saffman and Taylor [14] studied the slow penetration of water into a Hele-Shaw cell that was filled with oil, defining λ as the ratio of the diameter of the bubble to that of the tube. They presented relations among the bubble width, the viscous force and the surface tension. Since the front of the bubble is an asymptotic curve, the lines of the profile are not parallel up to 1.5 times the pipe diameter (3R). The diameter of the bubble is defined as its width measured at S = 3R. A formula that relates m, the pressure drop across the bubble, and Ca has been proposed Bretherton [2].

Taylor [17] obtained a curve of the fractional coverage as a function of the Ca using circular tubes with three diameters and various fluids. Three possible fluid flow patterns were predicted two re-circulating flows with a low Ca at $m < 0.5$ and one by-pass flow with a high Ca at $m > 0.5$. Cox [3, 4] found a numerical solution to the momentum equations for bubble motion by neglecting the gravity and inertia terms. They revealed that m asymptotically approaches $m = 0.6$, which is close to the value $m = 0.55$ that was estimated in Taylor's experiment, as Ca approaches 10. Their observations reveled that the final size and shape are reached at a position that 1.5 diameters away from the tip of the front tip of the bubble. Pitts [13] reported a theoretical shape equation of the bubble front for λ (the ratio of the bubble width to the inner diameter of the tube) smaller than 0.77, which is the maximum value which fits the experimental results.

Schwartz *et al.* [16] found that λ is a function of Ca, by obtaining the profile of the bubble and the residual fluid in a capillary. Their finding was consistent with that of Taylor

Fig. 1. Experimental system.

Table 1. Characteristics of silicone oil.

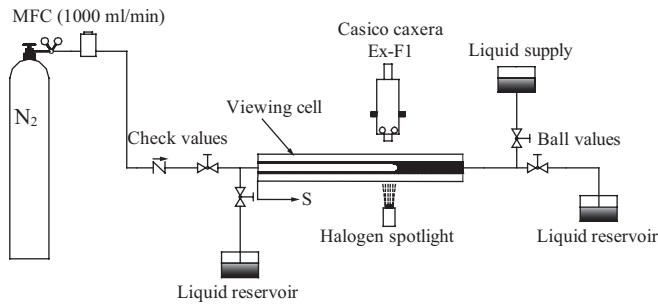| Viscosity 25°C (mm^2/sec)	Specific weight 25°C	Surface tension (mN/m)
1cs	0.818	16.9
5cs	0.915	19.7
10cs	0.935	20.1
50cs	0.960	20.8
100cs	0.965	20.9
1000cs	0.970	21.2
5000cs	0.975	21.3
10000cs	0.975	21.3
30000cs	0.976	21.3

[17]. Kolb and Cerro [10] found that m asymptotically approaches $m = 0.64$, which is close to the asymptotic value $m = 0.6$, suggested by Cox [4], at a higher Ca, by observing the long bubble in a square tube that was filled with a Newtonian fluid.

Huzyak and Koelling [9] experimentally determined that m is only related to Ca for Newtonian fluids, but is a function of both the Ca and the inner diameter of the tube for viscoelastic fluids.

Hsu *et al.* [7] observed the phenomenon of a long bubble stretching in a circular tube filled with silicon oil. A pressurized airflow was injected into a long horizontal glass tube. The result reveals that as the bubble evolutes in the tube, the velocity of bubble increases, however, the pressure decline gradually.

Salman *et al.* [15] observed the bubble formation in a vertical tube for air − water and air − octane systems. The gas flow was controlled by mass flow controller (MFC). Liao and Zhao [11] proposed a theoretical model to predict the drift velocity of Taylor bubble in vertical mini triangular and square channels. Zhao and Bi [19] observed the bubble in vertical equilateral triangular channels with three various hydraulic diameters. Bi and Zhao [1] observed the continuous variations of the bubble in vertical circular, triangular and rectangular tubes with various dimensions.

According to the experiment of Salman *et al.* [15], in this experiment, the volume rate of the injection gas was controlled by a mass flow controller (MFC). The profile and the evolution of the bubble were observed and compared for various volume flow rates of the injection gas, diameters of the entrance and viscosities of the liquid. The effects of the flow rate and the viscosity of the silicone oil on the velocity (U) and some dimensionless parameters, defined in Section 2.2, are studied.

II. EXPERIMENT

1. Experimental Setup

Fig. 1 schematically depicts this experimental system. It is modified from one adopted elsewhere by Huzyak and Koelling [9]. The images of the bubble are captured by a high-velocity camera (CASIO EX-F1) with 6 Mega pixel/60

frames per second. The light source is a coaxial light source (LA180-Me). The pressure at the entrance is 10 kg/cm^2. Nitrogen with 99.99% purity is selected as the injection gas. The volume rate of injection gas was controlled using a MFC (Brooks 5850E). The features of the MFC are: the range of flow rate is from 3 Sccm to 30 Slpm, the maximum inlet pressure is 150 psig (Max 1500 psig), the normal operating pressure range is from 5 to 50 psid, the accurate selection (analog) is ± 1.0% of F.S, the repeatability is ± 0.25% of F.S, the reaction time of flow signal is less than 0.3 sec, the temperature coefficient is ± 0.1% F.S/°C (N2), the normal operating temperature is ranged from 5°C to 65°C.

The gas was injected at three volume rates 1000 ml/min, 800 ml/min and 600 ml/min. The diameters of the entrance in this experiment were 7 mm, 5 mm and 3 mm. The tube was made of high-hardness heat-resistant glass, with a length of 1000 mm length and an interior diameter of 9 mm. The glass frame had dimensions 50 mm × 50 mm × 1000 mm, and the gap between the frame and the tube was filled with glycerin to reduce the effect of refraction. A ruler was fixed to the frame for convenience of calculation of the velocity of the bubble. The viscosity of the silicone oil ranged from 1cs to 1000cs. Table 1 presents the characteristics of the silicone oil.

2. Experimental Method

In this experiment, the evolution of the bubbles is recorded continuously using a CASIO EX-F1 camera. The tube is filled with silicone oil of various viscosities in an isothermal environment. The entrance orifices have three diameters - 7 mm, 5 mm and 3 mm. The profile of the bubble in each case is captured using a high-velocity camera.

The accuracy of measurement is confirmed using the method of Yamamoto [18]. The weight of the fluid that is expelled by the bubble is denoted w. The m of the bubbles is given by $m = 1 - \dfrac{w}{\rho \pi R_o^2 L}$. Where R_o is the radius of the tube, L is the length of the tube.

This study investigates the effects of flow rate and viscosity of silicone oil on the bubble velocity and the dimen-
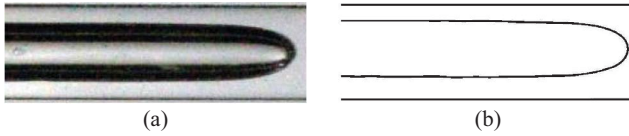
(a)　　　　　　　　　　　　　　　(b)

Fig. 2. Bubble image before and after processing.

sionless parameters *Ca*, *Re*, λ and *m*. The dimensionless parameters are defined as follows.

$$Ca = \frac{U \times \eta}{\sigma} \qquad (1)$$

$$Re = \frac{\rho \times U \times D}{\eta} \qquad (2)$$

$$\lambda = \frac{R_b}{R_o} \qquad (3)$$

$$m = \frac{R_o - R_b}{R_o} = 1 - \lambda^2 \qquad (4)$$

3. Image Processing Method

In this study, the photographs captured by the camera are processed using the image post-processing program written in MATLAB, to measure the dimensions of the bubble accurately. The fractional converge (m) was estimated from these photographs. Fig. 2(a) presents a photograph before image processing and the ultimate graphics generated by the image processing. Binarization and skeletonization are adopted to eliminate the errors caused by the light. The bubble profile obtained by the Level Set Method [8], are shown in Fig. 2(b). The width of the bubble is estimated from this profile.

III. RESULTS AND DISCUSSION

1. Effects of Viscosity on Bubble Velocity

The literature does not cover the effects of viscosity on the bubble velocity, which is investigated herein. The MFC controls the gas flow; the inlet pressure is 10 kg/cm^2, and the diameter of the entrance orifice is 9 mm. Figs. 3-5 plot the dynamic characteristic of bubble velocity, corresponding to the locations associated with gas flow rates of 600 ml/min, 800 ml/min and 1000 ml/min, respectively. The results show that the velocity of the bubble increases with the viscosity of the fluid and the flow rate of the gas. The rate of change of velocity in silicone oil is high in the range 500cs to 1000cs. The bubble velocity significantly increases along tube path in high-viscosity fluids. The bubble moves faster in fluid of higher viscosity at the rear of the tube but the opposite effect is evident at the front of the tube. A higher driving force is required to the drive a fluid of higher viscosity, and a higher bubble velocity is associated with a higher driving force for
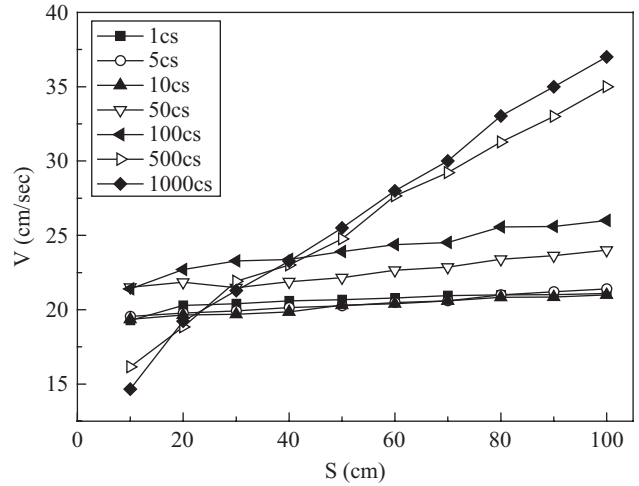

Fig. 3. Position of bubble front corresponds to the velocity of the bubble for Q = 600 ml/min.
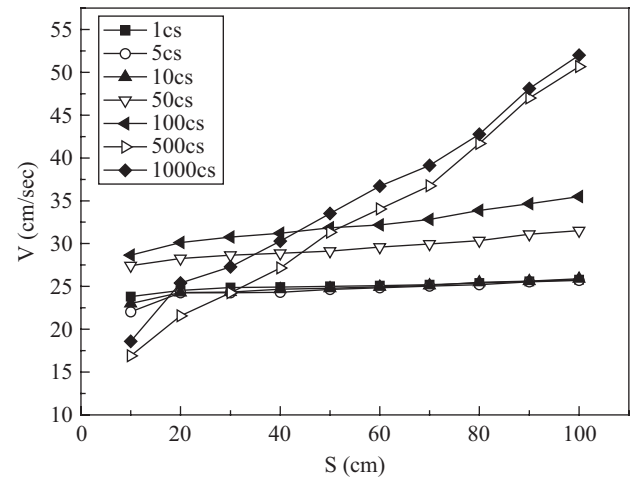

Fig. 4. Position of bubble front corresponds to the velocity of the bubble for Q = 800 ml/min.
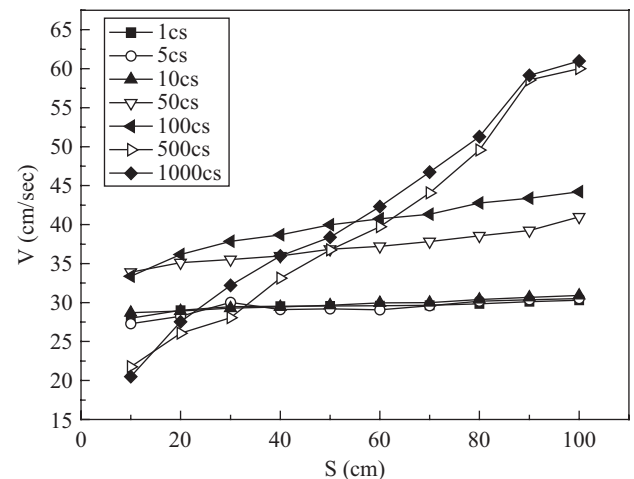

Fig. 5. Position of bubble front corresponds to the velocity of the bubble for Q = 1000 ml/min.

a given gas flow rate. The resistance increases with the fluid viscosity; the gas pressure at the entrance, provided by the MFC, and the acceleration of the driven gas also increase. This result consistent with the result of [7].

2. Effects of Gas Flow Rate, Entrance Diameter and Viscosity of Fluid

Silicone oils with three viscosities, 100cs, 500cs and 1000cs, are used for comparison in this experiment. Figs. 6-8 plot the bubble velocity for silicone oils with these three viscosities. The dynamic characteristics of the bubble velocity are compared by varying the entrance diameters, 3 mm, 5 mm, 7 mm and 9 mm, and the gas flow rate, 600 ml/min, 800 ml/min and 1000 ml/min.

Fig. 6 pots the effects of the flow rate and the entrance diameter on the bubble velocity in silicone oil with a viscosity of 100cs. The bubble velocity increases with the gas flow rate. The entrance effects, shown Fig. 6, are evident adjacent to the entrance, from S = 0 cm to S = 20 cm. A higher bubble velocity is associated with a smaller diameter of the entrance for the same flow rate. The bubble velocity increases markedly at the entrance length as the diameter of the entrance or the viscosity fluid declines. For a fixed flow rate, a smaller entrance diameter corresponds to a faster bubble. However, changes in the diameter of the entrance aperture have less effect on the bubble velocity from 30 cm to the exit. Therefore, the flow rate of the injected gas mainly affects the bubble velocity at the entrance.

Figs. 7 and 8 indicate that effect on the bubble velocity of the flow rate of the injected gas or the entrance diameter is minor in high-viscosity fluids. As stated above, the bubble velocity increases as the entrance diameter declines for a constant flow rate, controlled using the MFC. The entrance effects dominate in low-viscosity silicone oil or when the entrance has a small diameter, but they are weak in high-viscosity fluids.

3. Effect on Dimensionless Parameters

The relationship between the dimensionless parameters is studied under the following conditions. The entrance pressure is 10 kg/cm^2, the diameter of the entrance aperture is 9 mm and the gas flow rate is 1000 ml/min. A high-velocity camera is set up above the middle of the circular tube (at S = 50 cm). The width of the bubble is measured at a position 1.5 diameter from the back of the bubble using some image-processing methods.

Fig. 9 plots the relationship between *Ca* and *m* for silicone oil with various viscosities. The results show that when the viscosity of the fluid is less than 500cs, *m* increases with *Ca*. However, when the viscosity exceeds 500cs, *m* is approximately fixed at approximately 0.6. The value of *m* remains 0.6 for any *Ca* of greater than 10. This result agrees with the prediction of Cox [3]. When the viscosity of the fluid is less than 500cs, *m* monotonically increases with increasing viscosity. The width of the bubble and the curva-
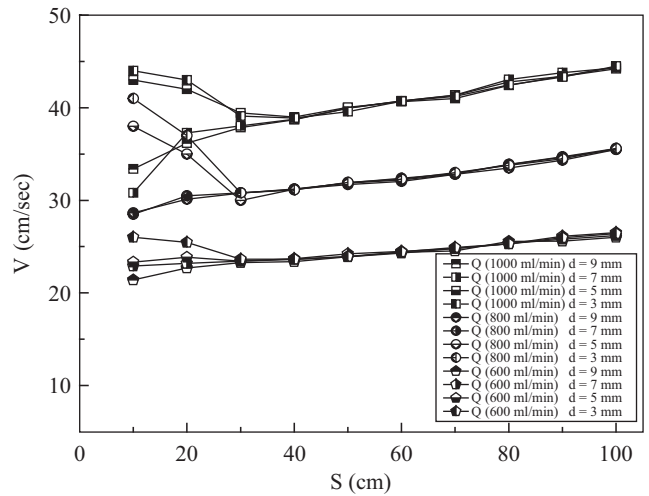

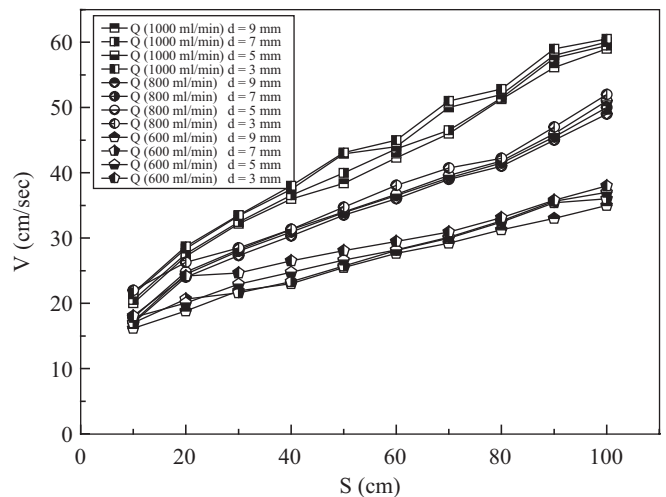**Fig. 6. Entrance effects in silicone oil with viscosity of 100cs.**

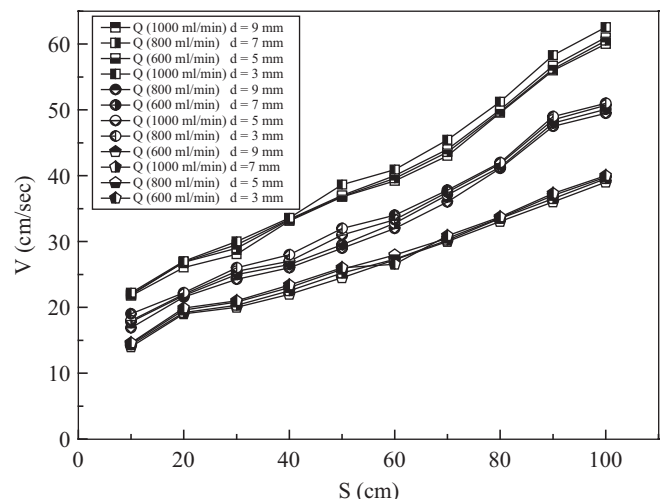**Fig. 7. Entrance effects in silicone oil with viscosity of 500cs.**

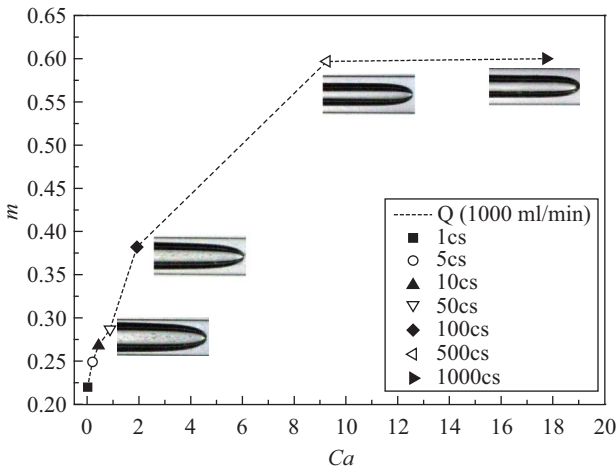**Fig. 8. Entrance effects in silicone oil with viscosity of 1000cs.**

Fig. 9. *Ca* **versus** *m* **for silicone oil with various viscosities for Q = 1000 ml/min.**
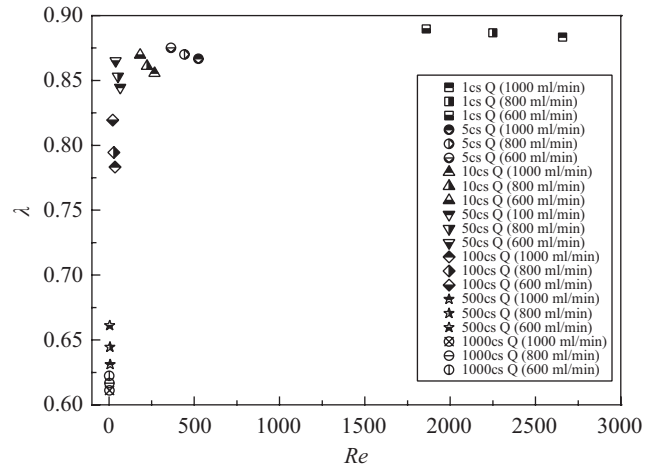

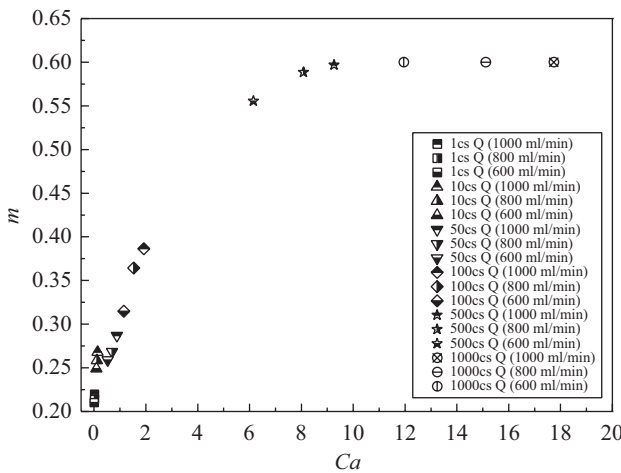**Fig. 11.** *Re* **versus** *λ* **for various gas flow rates through silicone oil of various viscosities.**

Fig. 10. *Ca* **versus** *m* **for various gas flow rates and silicone oil of various viscosities.**

Fig. 12. *Ca* **versus** *m* **for 100cs silicone oil.**

Fig. 13. *Re* **versus** *λ* **for 100cs silicone oil.**

ture at its tip increase, as the viscosity declines. A particular bubble shape is maintained as the viscosity exceeds 500cs is m remains constant.

Fig. 10 plots the relationship between *Ca* and *m* for silicone oils with various viscosities and flow rates. For a given viscosity, *Ca* and *m* increase with the gas flow rate. The variation of *m* is lower at high viscosity 500cs and low viscosity (less than 50cs). In 100cs silicone oil, the variation of *m* (0.076) with flow rate from 600 ml/min to 1000 ml/min is greatest. The gas flow rate clearly affects *Ca* of the high-viscosity fluid. *Ca* increases from 6 to 10 as the flow changes from 600 ml/min to 1000 ml/min for silicone oil with a viscosity of 500cs. However, *Ca* changes from 12 to 18 for silicone oil with a viscosity 1000cs viscosity for the same variation in flow rate. Clearly, the gas flow rate affects *Ca* in high-viscosity silicone oil and the strength of the effect increases with the viscosity of the oil.

Fig. 11 plots the relationship between *Re* and *λ* for dif-
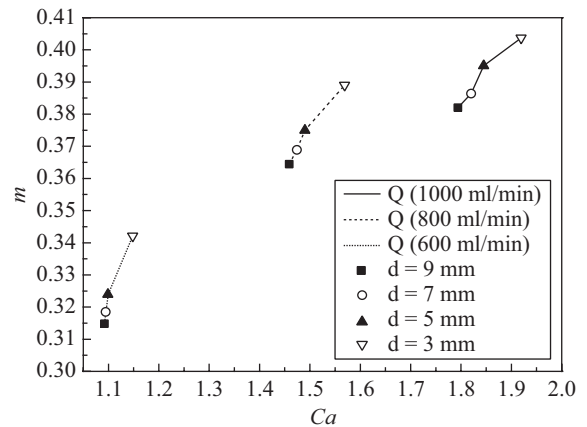
ferent viscosities and gas flow rates. It shows *Re* increases as the viscosity of the silicone oil decreases. The largest variation in *Re* with mass flow rate occurs when the viscosity is less than 5cs. However, when the fluid viscosity exceeds
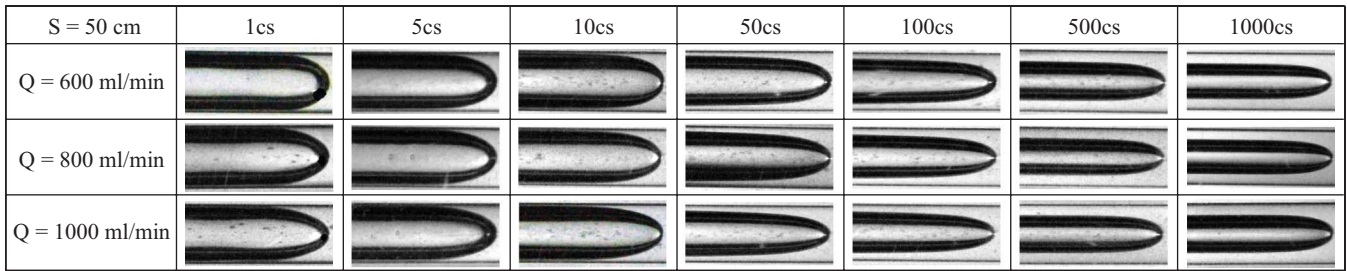
S = 50 cm	1cs	5cs	10cs	50cs	100cs	500cs	1000cs
Q = 600 ml/min							
Q = 800 ml/min							
Q = 1000 ml/min							

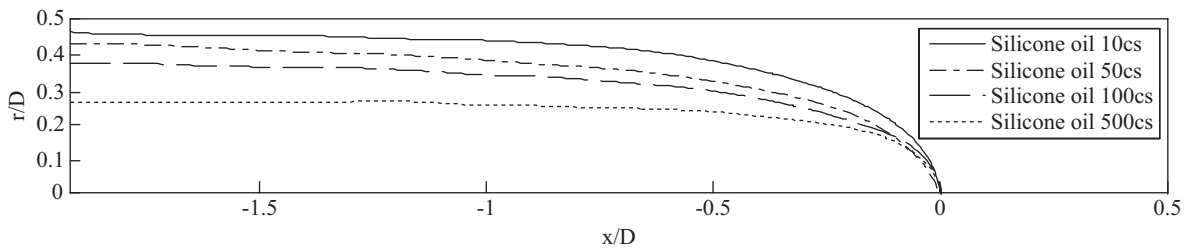**Fig. 14. Bubble contours in silicone oil of various viscosities.**

Fig. 15. Evolution of bubble contours for silicone oil of various viscosities, after image processing.

50cs, *Re* approaches a low value, but λ varies greatly from 0.64 to 0.86. For a particular viscosity of the fluid, the bubble grows larger as λ increases with a drop in the gas flow rate. The largest value of λ is close to 0.88, obtained when the viscosity is 1cs and the flow rate is 600 ml/min. Pitts [13] predicted the bubble profile for $\lambda = 0.88$.

The relationships between *Ca* and *m* and between *Re* and λ for different diameters of the entrance aperture and different flow rates are studied using 100cs viscosity silicone oil. Figs. 12 and 13 present the results. Fig. 12 indicates that both *Ca* and *m* increase with the gas flow rate (Q). The value of m increases as the diameter of the entrance declines for the same gas flow rate. Increasing *m* reduces the width of the bubble.

Fig. 13 indicates that *Re* increases with the gas flow rate. However, λ declines as the gas flow rate increases. The value of λ also declines along as the entrance diameter declines for a given gas flow rate. At lower λ, a smaller bubble is formed. The greatest variation in the *m* and λ values occurs as the diameter is varied from 3 mm to 5 mm. Reducing the entrance diameter and increasing the flow rate increase *Ca*, *m*, and *Re* and reduce λ, as determined by comparing Figs. 12 and 13.

4. Effects of Various Viscosities on Bubble Profiles

Fig. 14 presents images of bubble profiles in silicone oil with various viscosities. The bubble front has a sharper tip, a smaller radius of curvature, as the gas flow rate injected into the silicone oil is increased below 100cs. The bubble width declines as the viscosity increases for a given gas flow rate. The photographs in Fig. 14 were obtained using an image processing program that was written in the Matlab. The bubble profile is using the Level Set Method [8]. Fig. 15 presents the dimensionless bubble profiles.

Fig. 16 shows the bubble development for various injecttion diameters for two viscosities. The rate of growth of the bubble grows increases as the fluid viscosity declines, for a given diameter of the entrance. The bubble in the low-viscosity fluid has no obvious tip when the diameter of the entrance is 5 mm or 7 mm. Comparing the photographs of bubble evolution indicates that the velocity of the bubble increases with the diameter of the entrance.

Figs. 17 and 18 and Table 2 present the time required for a bubble to grow to its final shape. The gas flow rate is set to 600 ml/min. The profile of the bubbles and the time spent at positions S = 4 cm and S = 15 cm are shown. Comparing the photographs, in Figs. 17 and 18, of the bubble in the 100cs fluid indicates that the bubble injected through the smaller diameter d = 3 mm, reaches the position S = 4 cm later, but it reaches the position S = 15 cm sooner. The acceleration of this bubble exceeds that of other two bubbles from S = 4 cm to S = 15 cm. Therefore, this bubble catches up, or even overtakes the other two bubbles. Similarly, the photograph of the 500cs fluid supports the same conclusion. The bubble profiles in the 100cs fluid and the 500cs fluid are compared at the position S = 4 cm for the 7 mm entrance. The tip is sharper in the100cs fluid than in the 500cs fluid. For a given flow rate, a smaller diameter of injection requires the gas to spend more time to overcome the inertial force of the silicone oil, but it then accelerates faster. The shape of the bubble front changes from a sharp tip to a blunt one as the viscosity increases.

The profiles of the bubbles generated from entrances of various diameters are very similar at S = 15 cm in fluids with the same viscosity. Therefore, these bubbles are in the steady state. Comparing the contours of these bubbles, it shows that a lower viscosity fluid contains wider bubbles.
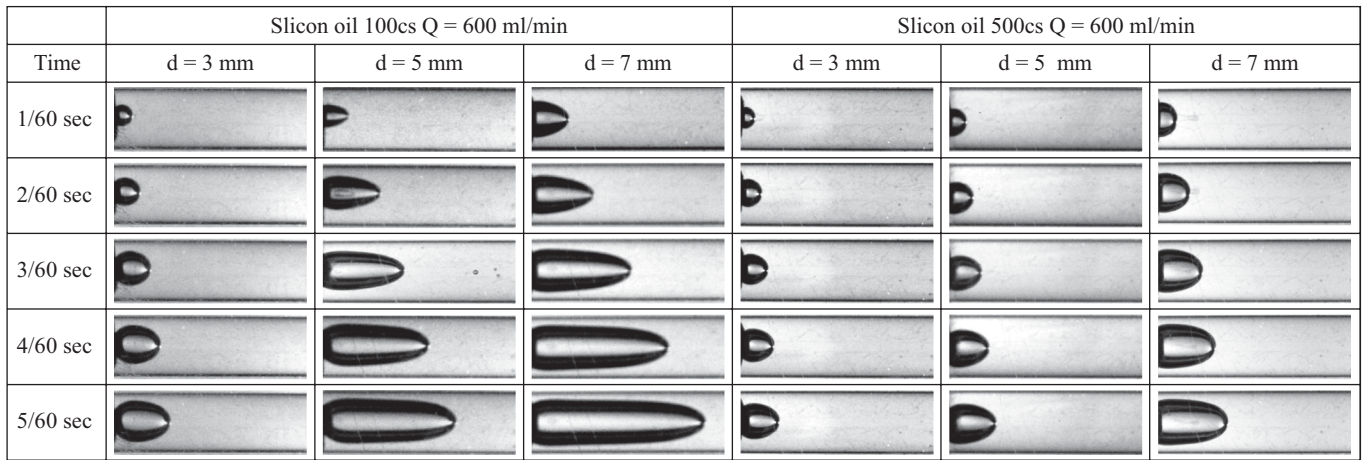
Time	Silicon oil 100cs Q = 600 ml/min			Silicon oil 500cs Q = 600 ml/min		
	d = 3 mm	d = 5 mm	d = 7 mm	d = 3 mm	d = 5 mm	d = 7 mm
1/60 sec						
2/60 sec						
3/60 sec						
4/60 sec						
5/60 sec						

Fig. 16. **Initial bubble contours following injection through entrances of various diameters in silicone oil of various viscosities.**

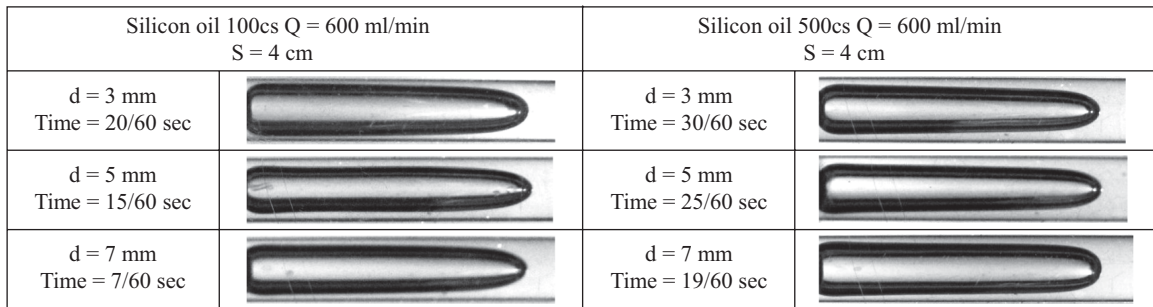| Silicon oil 100cs Q = 600 ml/min S = 4 cm		Silicon oil 500cs Q = 600 ml/min S = 4 cm	
d = 3 mm Time = 20/60 sec		d = 3 mm Time = 30/60 sec	
d = 5 mm Time = 15/60 sec		d = 5 mm Time = 25/60 sec	
d = 7 mm Time = 7/60 sec		d = 7 mm Time = 19/60 sec	

Fig. 17. **Time-evolution of contours of bubble grown to S = 4 cm for different entrance diameters.**

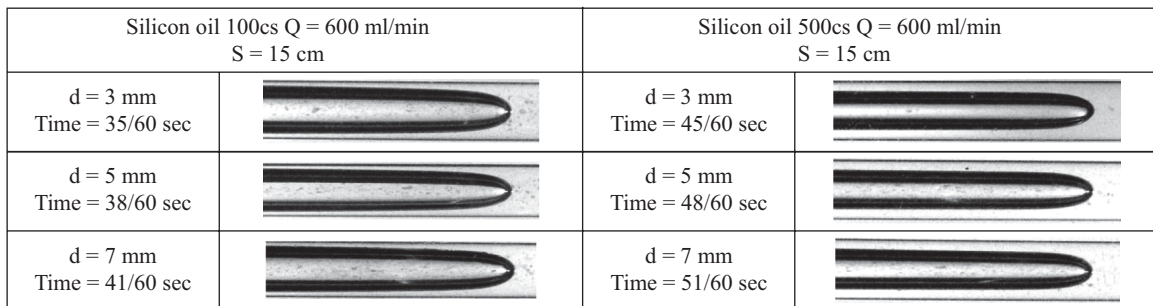| Silicon oil 100cs Q = 600 ml/min S = 15 cm		Silicon oil 500cs Q = 600 ml/min S = 15 cm	
d = 3 mm Time = 35/60 sec		d = 3 mm Time = 45/60 sec	
d = 5 mm Time = 38/60 sec		d = 5 mm Time = 48/60 sec	
d = 7 mm Time = 41/60 sec		d = 7 mm Time = 51/60 sec	

Fig. 18. **Time-evolution of contours of bubbles grown to S = 15 cm for different entrance diameters.**

5. Error Analysis

Table 3 shows the difference of average velocity of bubble front in the tube filled with various viscosity silicone oil. The observation ranges are 50-55 cm and 50-60 cm. The flow rate is Q = 1000 ml/min. The average velocity calculated from the bubble front moving distance divided by the time interval obtained from 1/60 sec each photograph frame. Because the differences of average velocity are less than 0.2%, the average speed of the bubble front calculated with the span of 10 cm in our experiment.

Table 4 shows the difference of fractional converges obtained by MATLAB and pixel scale method as the flow rate is Q = 1000 ml/min for various viscosity silicone oil. Each photograph pixel can be converted into 0.038 mm, because the photograph of the tube profile is captured by the camera from tube with 9 mm diameter. The pixel scale method estimates the diameters of profiles bubble by converting each pixel into 0.038 mm. The width of the bubbles was estimated from these images. Furthermore, the bubble profiles, which are obtained by the Level Set Method [8]. The width of the bubbles are estimated from these profiles. Because the differences of average velocity are less than 0.45%, the fractional converges calculated with MATLAB in our experiment.
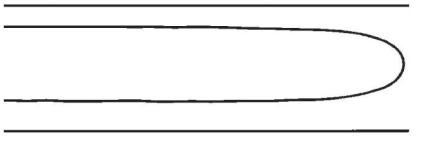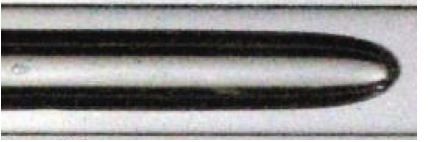
Table 2. Lengths of grown bubbles at various times.

Diameter (mm)	Silicone oil 100cs Q = 600 ml/min		Silicone oil 500cs Q = 600 ml/min	
	Time (sec)		Time (sec)	
	S = 4 cm	S = 15 cm	S = 4 cm	S = 15 cm
d = 3	20/60	35/60	30/60	45/60
d = 5	15/60	38/60	25/60	48/60
d = 7	7/60	41/60	19/60	51/60

Table 3. The error analysis of bubble average velocity.

Viscosity of silicone oil	Average velocity (unit: cm/sec) at each shoot location (Q = 1000 ml/min)				
	Number of pictures captured at 50-55 cm	Number of pictures captured at 50-60 cm	50-55 cm	50-60 cm	Difference of average velocity (%)
1cs	10	19	29.10	29.15	0.17
5cs	10	19	29.30	29.34	0.13
10cs	10	19	29.78	29.84	0.20
50cs	9	19	39.68	39.74	0.15
100cs	7	14	40.44	40.50	0.14
500cs	6	13	40.63	40.7	0.17
1000cs	5	12	42.25	42.3	0.11

Table 4. The error analysis of bubble image process.

Viscosity of silicone oil	Bubble image captured at position S = 50 cm in D = 9 mm tube (Q = 1000 ml/min)		
	Fractional converge by using MATLAB	Fractional converge by using pixel scale method	Average error of fractional converge (%)
1cs	0.219	0.218	0.45
5cs	0.248	0.249	0.40
10cs	0.268	0.267	0.37
50cs	0.286	0.287	0.34
100cs	0.382	0.381	0.26
500cs	0.596	0.597	0.18
1000cs	0.601	0.602	0.16

IV. CONCLUSION

The velocity of a bubble typically increases as the flow rate increases or the diameter of the entrance declines. The velocity of the bubble increases with the inlet pressure and the viscosity of the silicone oil at a constant flow rate. The effect of the entrance diameter on the velocity of the bubble is greater in lower viscosity, and is weak at high viscosity. As the gas flow rate increases, the Capillary number and the Reynolds number also increase, given constant viscosity. How-

ever, the hollow ratio declines as while flow rate increases. The fractional converge is close to 0.6 when *Ca* approaches 10 and the silicone oil has a viscosity of 500cs. This result agrees with the prediction of Cox.

In silicone oil with under 100cs viscosity, the bubbles grow faster and have a more cuspate shape; it undergoes greater acceleration and meets less fluid resistance for the same volume flow rate. The bubble, generated at the entrance with the small diameter, takes more time to reach the same position, and so the evolution velocity of the bubble in the front of the

tube is low. The bubble profile appears to be blunt when the gas is injected into the silicone oil with a high viscosity through an entrance with a large diameter.

ACKNOWLEDGMENTS

NOMENCLATURE

Ca	capillary number
D	diameter of circular tube
Re	reynolds number
R_b	radius of bubble
R_o	radius of circular tube
m	fractional converge
U	average velocity of bubble

Greek Letters

η	viscosity of silicone oil
σ	surface tension of silicone oil
ρ	density of silicone oil
λ	hollow ratio

REFERENCES

1. Bi, Q. C. and Zhao, T. S., "Taylor bubble in miniaturized circular and noncircular channels," *International Journal of Multiphase Flow*, Vol. 27, pp. 561-570 (2001).
2. Bretherton, F. P., "The motion of long bubbles in tubes," *Journal of Fluid Mechanics*, Vol. 10, pp. 166-188 (1961).
3. Cox, B. G., "On driving a viscous fluid out of a tube," *Journal of Fluid Mechanics*, Vol. 14, pp. 81-96 (1962).
4. Cox, B. G., "An experimental investigation of the streamlines in viscous fluids expelled from a tube," *Journal of Fluid Mechanics*, Vol. 20, pp. 193-200 (1964).
5. Fairbrother, F. P. and Stubbs, A. E., "Studies in electroendosmosis. Part VI. The bubble tube method of measurement," *Journal of Chemical Society*, Vol. 1, pp. 527-529 (1935).
6. Hargrove, J., "Supercavitation and aerospace technology in the development of high-speed underwater vehicles," *42nd AIAA Aerospace Sciences Meeting and Exhibit*, pp. 3547-3555 (2004).
7. Hsu, C. H., Kung, K. Y., Chen, P. C., and Hu, S. Y., "Experimental visualization of gas-assisted injection long bubble in a tube," *WSEAS Transactions on Applied and Theoretical Mechanics*, Vol. 4, No. 1, pp. 1-10 (2009).
8. Hsu, C. H., Kuo, C. C., Chang, C. C., and Kung, K. Y., "The study on the asymptotic profile and the flow patterns in front of along bubble through a circular tube," *Journal of Marine Science and Technology*, Vol. 18, No. 6, pp. 860-866 (2010).
9. Huzyak, P. C. and Koelling, K. W., "The penetration of a long bubble through a viscoelastic fluid in a tube," *Journal of Non-Newton Fluid Mechanics*, Vol. 71, pp. 73-88 (1997).
10. Kolb, W. B. and Cerro, R. L., "Coating the inside of a capillary of square cross section," *Chemical Engineering Science*, Vol. 46, pp. 2181-2195 (1991).
11. Liao, Q. and Zhao, T. S., "Modeling of Taylor bubble rising in a vertical mini non-circular channel filled with a stagnant liquid," *International Journal of Multiphase Flow*, Vol. 29, pp. 411-434 (2003).
12. Ong, N. S., Lee, H. L., and Parvez, M. A., "Influence of processing conditions and part design on the gas-assisted injection molding process," *Advances in Polymer Technology*, Vol. 20, No. 4, pp. 270-280 (2001).
13. Pitts, E., "Penetration of fluid into a Hele-Shaw cell: the Saffman-Taylor experiment," *Journal of Fluid Mechanics*, Vol. 97, pp. 53-64 (1980).
14. Saffman, P. G. and Taylor, G. I., "The penetration of a fluid into a porous medium or Hele-Shaw cell containing a more viscous liquid," *Proceedings of Royal Society A*, Vol. 245, pp. 312-329 (1958).
15. Salman, W., Gavriilidis, A., and Angeli, P., "On the formation of Taylor bubbles in small tubes," *Chemical Engineering Science*, Vol. 61, pp. 6653-6666 (2006).
16. Schwartz, L. W., Princen, H. M., and Kiss, A. D., "On the motion of bubbles in capillary tubes," *Journal of Fluid Mechanics*, Vol. 172, pp. 259-275 (1986).
17. Taylor, G. I., "Deposition of a viscous fluid on the wall of a tube," *Journal of Fluid Mechanics*, Vol. 10, pp. 161-165 (1960).
18. Yamamoto, T., Suga, T., Nakamura, K., and Moti, N., "The gas penetration through viscoelastic fluid with shear-thinning viscosity in a tube," *Transactions of the ASME*, Vol. 126, pp. 148-152 (2004).
19. Zhao, T. S. and Bi, Q. C., "Co-current air-water two-phase flow patterns in capillary triangular channels," *International Journal Multiphase Flow*, Vol. 27, pp. 765-782 (2001).